LETTER

doi:10.1038/nature10357

The ageing systemic milieu negatively regulates neurogenesis and cognitive function

Saul A. Villeda[1,2], Jian Luo[1], Kira I. Mosher[1,2], Bende Zou[3], Markus Britschgi[1]†, Gregor Bieri[1,4], Trisha M. Stan[1,5], Nina Fainberg[1], Zhaoqing Ding[1,5], Alexander Eggel[1], Kurt M. Lucin[1], Eva Czirr[1], Jeong-Soo Park[1]†, Sebastien Couillard-Després[6], Ludwig Aigner[6], Ge Li[7], Elaine R. Peskind[7,8], Jeffrey A. Kaye[9], Joseph F. Quinn[9], Douglas R. Galasko[10], Xinmin S. Xie[3], Thomas A. Rando[1,11,12] & Tony Wyss-Coray[1,2,5,11]

In the central nervous system, ageing results in a precipitous decline in adult neural stem/progenitor cells and neurogenesis, with concomitant impairments in cognitive functions[1]. Interestingly, such impairments can be ameliorated through systemic perturbations such as exercise[1]. Here, using heterochronic parabiosis we show that blood-borne factors present in the systemic milieu can inhibit or promote adult neurogenesis in an age-dependent fashion in mice. Accordingly, exposing a young mouse to an old systemic environment or to plasma from old mice decreased synaptic plasticity, and impaired contextual fear conditioning and spatial learning and memory. We identify chemokines—including CCL11 (also known as eotaxin)—the plasma levels of which correlate with reduced neurogenesis in heterochronic parabionts and aged mice, and the levels of which are increased in the plasma and cerebrospinal fluid of healthy ageing humans. Lastly, increasing peripheral CCL11 chemokine levels *in vivo* in young mice decreased adult neurogenesis and impaired learning and memory. Together our data indicate that the decline in neurogenesis and cognitive impairments observed during ageing can be in part attributed to changes in blood-borne factors.

Adult neurogenesis occurs in local microenvironments, or neurogenic niches, in the subventricular zone (SVZ) of the lateral ventricles and the subgranular zone (SGZ) of the hippocampus[2,3]. Permissive cues within the neurogenic niche are thought to drive the production of new neurons and their subsequent integration into the neurocircuitry of the brain[4,5], directly contributing to cognitive processes including learning and memory[6–9]. Importantly, the neurogenic niche is localized around blood vessels[10,11], allowing for potential communication with the systemic environment. Therefore, the possibility arises that diminished neurogenesis during ageing may be modulated by the balance of two independent forces: intrinsic central nervous system (CNS)-derived cues[12–14] and cues extrinsic to the CNS delivered by blood. Thus we hypothesized that age-related systemic molecular changes could cause a decline in neurogenesis and impair cognitive function during ageing.

We first characterized cellular, electrophysiological and behavioural changes associated with the neurogenic niche in the dentate gyrus of the hippocampus in an ageing cohort of mice. We observed cellular changes consistent with markedly decreased adult neurogenesis[1] and increased neuroinflammation with age[15] (Supplementary Fig. 2a–e). Additionally, we detected deficits in synaptic plasticity (Supplementary Fig. 3a–c), and behavioural deficits in contextual fear conditioning (Supplementary Fig. 4a–c) and radial arm water maze (RAWM; Supplementary Fig. 4d–f) paradigms in old animals, consistent with decreased cognitive function during ageing[16].

Next we investigated the contribution of peripheral systemic factors to the age-related decline in neurogenesis in the dentate gyrus of the hippocampus in the setting of isochronic (young–young and old–old) and heterochronic (young–old) parabiosis (Fig. 1a). Remarkably, the number of doublecortin (Dcx)-positive newly born neurons (Fig. 1b, c), BrdU-positive cells (Fig. 1e, f) and Sox2-positive progenitors (Supplementary Fig. 5a, b) decreased in young heterochronic parabionts. In contrast, we observed an increase in the number of Dcx-positive (Fig. 1b, d), BrdU-positive (Fig. 1e, g) and Sox2-positive (Supplementary Fig. 5a, c) cells in the old heterochronic parabionts. The number of Dcx-positive neurons between unpaired age-matched animals and isochronic animals showed no difference (Supplementary Fig. 6a, b). As a control, flow cytometry analysis confirmed a shared vasculature in a subset of parabiotic pairs, in which one parabiont was transgenic for green fluorescent protein (GFP; Supplementary Fig. 7a–d). Together our findings suggest that global age-dependent systemic changes can modulate neurogenesis in both the young and aged neurogenic niche, potentially contributing to the decline in regenerative capacity observed in the normal ageing brain.

As previously reported by others[17], we rarely detected peripherally derived GFP cells in the CNS of wild-type mice, and these numbers did not differ between isochronic and heterochronic pairings (Supplementary Fig. 7e), suggesting that the observed effects are mediated by soluble factors in plasma. To confirm that circulating factors within aged blood contribute to reduced neurogenesis with age, we intravenously injected plasma isolated from young or old mice into young adult mice (Fig. 2a). The number of Dcx-positive cells in the dentate gyrus decreased in animals receiving old plasma compared to animals receiving young plasma (Fig. 2b, c), indicating that soluble factors present in old blood inhibit adult neurogenesis.

To investigate the functional effect of the ageing systemic milieu, extracellular electrophysiological recordings were done on hippocampal slices prepared from young isochronic and heterochronic parabionts (Fig. 1h, i and Supplementary Fig. 6c). A decrease in long-term potentiation (LTP) in the dentate gyrus of heterochronic parabionts was detected (Fig. 1h, i). These data indicate that age-related systemic changes can elicit deficits in synaptic plasticity. As LTP is considered to be a correlate of learning and memory[18], these finding suggest that age-related systemic changes may also affect cognitive functions during ageing.

[1]Department of Neurology and Neurological Sciences, Stanford University School of Medicine, Stanford, California 94305, USA. [2]Neuroscience IDP Program, Stanford University School of Medicine, Stanford, California 94305, USA. [3]AfaSci Research Laboratory, Redwood City, California, 94063, USA. [4]School of Life Sciences, Swiss Federal Institute of Technology (EPFL), CH-1015 Lausanne, Switzerland. [5]Immunology IDP Program, Stanford University School of Medicine, Stanford, California 94305, USA. [6]Institute of Molecular Regenerative Medicine, Paracelsus Medical University, Strubergasse 21, A-5020 Salzburg, Austria. [7]Department of Psychiatry and Behavioral Sciences, University of Washington School of Medicine, Seattle, Washington 98108-1597, USA. [8]Veterans Affairs Northwest Network Mental Illness Research, Education, and Clinical Center, Seattle, Washington 98108-1597, USA. [9]Layton Aging & Alzheimer's Disease Center, Oregon Health and Science University, CR131, 3181 SW Sam Jackson Park Road, Portland, Oregon 97201-3098, USA; and Portland VA Medical Center, Portland, Oregon 97207, USA. [10]Department of Neurosciences, University of California San Diego, 9500 Gilman Drive #0948, La Jolla, California 92093-0948, USA. [11]Center for Tissue Regeneration, Repair and Restoration, VA Palo Alto Health Care System, Palo Alto, California 94304, USA. [12]The Glenn Laboratories for the Biology of Aging, Stanford University School of Medicine, Stanford, California 94305, USA. †Present addresses: CNS Discovery, pRED, F. Hoffmann-La Roche Ltd., CH-4070 Basel, Switzerland (M.B.); Department of Biochemistry, College of Medicien, Dankook University, Cheonan 330-714, South Korea (J.S.P.).

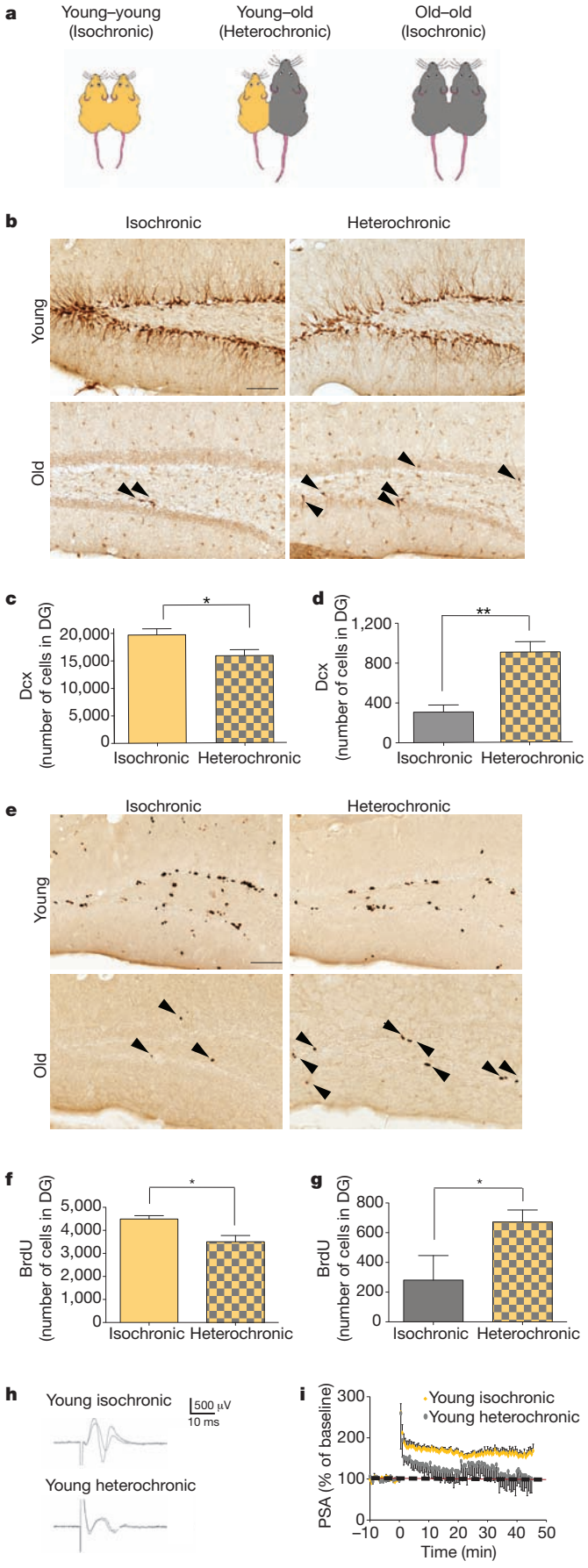

Figure 1 | Heterochronic parabiosis alters neurogenesis in an age-dependent fashion. **a**, Schematic showing parabiotic pairings. **b**, **e**, Representative fields of Dcx (**b**) and BrdU (**e**) immunostaining of young (3–4 months; yellow) and old (18–20 months; grey) isochronic and heterochronic parabionts 5 weeks after parabiosis (arrowheads point to individual cells; scale bars, 100 μm). **c**–**f**, Quantification of neurogenesis (**c**, **d**) and proliferating cells (**e**, **f**) in the young (**c**, **e**; top) and old (**d**, **f**; bottom) dentate gyrus (DG) after parabiosis. Data from 12 young isochronic, 10 young heterochronic, 6 old isochronic and 12 old heterochronic parabionts. **g**, **h**, Population spike amplitude (PSA) was recorded from the dentate gyrus of young parabionts. Representative electrophysiological profiles (**g**) and LTP levels (**h**) are shown for young heterochronic and isochronic parabionts. Data from 4–5 mice per group. All are data represented as mean + s.e.m.; $*P < 0.05$; $**P < 0.01$, *t*-test.

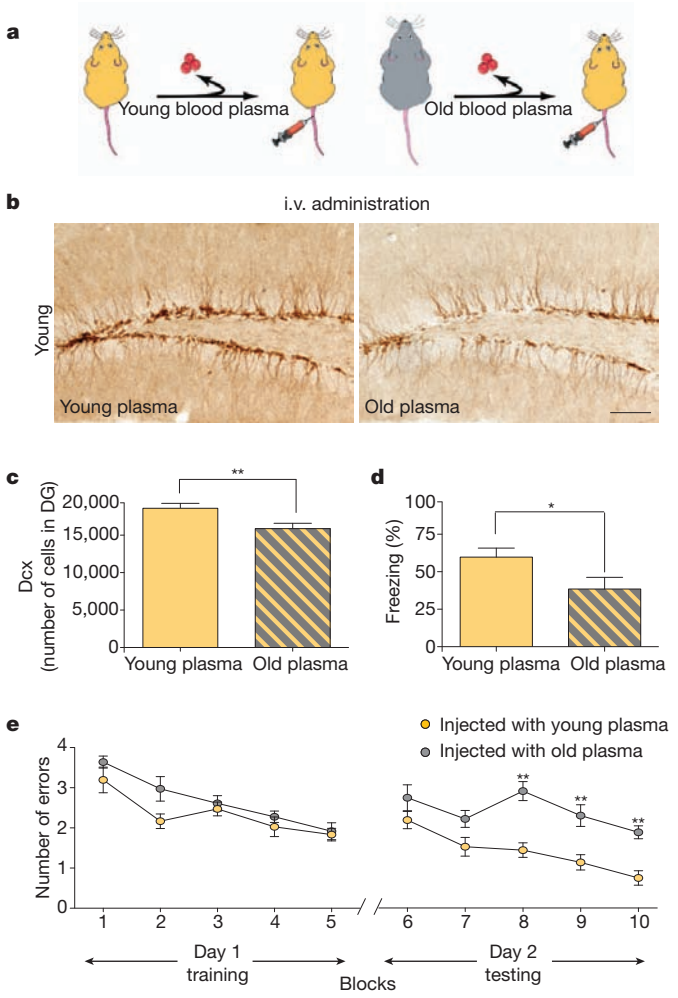

Figure 2 | Factors from an old systemic environment decrease neurogenesis and impair learning and memory. **a**, Schematic of young (3–4 months) or old (18–22 months) plasma extraction and intravenous (i.v.) injection into young (3 months) adult mice. **b**, Representative field of Dcx immunostaining of young adult mice after plasma injection treatment four times over 10 days (scale bar, 100 μm). **c**, Quantification of neurogenesis in the young dentate gyrus after plasma injection. Data from 8 mice injected with young plasma and 7 mice injected with old plasma. **d**, **e**, Hippocampal learning and memory assessed by contextual fear conditioning (**d**) and RAWM (**e**) paradigms in young adult mice after young or old plasma injections nine times over 24 days. **d**, Percent freezing time 24 h after training. Data from 8 mice per group. **e**, Number of entry arm errors before finding platform. Data from 12 mice per group. All data represented as mean ± s.e.m.; $*P < 0.05$; $**P < 0.01$, *t*-test (**c**, **d**), repeated measures ANOVA, Bonferroni post-hoc test (**e**).

Subsequently, we tested hippocampal-dependent learning and memory using contextual fear conditioning and RAWM paradigms in young adult mice intravenously injected with young or old plasma (Fig. 2d, e). During fear conditioning training mice exhibited no differences in baseline freezing regardless of plasma injection treatment (Supplementary Fig. 8a). However, mice receiving old plasma demonstrated decreased freezing in contextual (Fig. 2d), but not cued (Supplementary Fig. 8b), memory testing. During the training phase of the RAWM all mice showed similar swim speeds (Supplementary Fig. 8c) and spatial learning capacity for the task (Fig. 2e). However, during the testing phase animals that had received old plasma demonstrated impaired learning and memory for platform location (Fig. 2e). As a control, we tested the RAWM paradigm in young adult mice with ablated hippocampal neurogenesis and observed corresponding behavioural deficits (Supplementary Fig. 9a–e). Collectively, these data indicate that factors present in ageing blood inhibit adult neurogenesis, and functionally contribute to impairments in cognition.

Previous pioneering studies focused on muscle have shown that exposure of the aged stem cell niche to a young systemic environment through heterochronic parabiosis results in increased regeneration after muscle injury[19], in part by involving Notch signalling[28]. However, individual systemic factors associated with ageing and tissue degeneration have not yet been characterized or investigated for their role in regulating the decline in tissue regeneration. To identify such factors, we used a proteomic approach in which relative levels of 66 cytokines, chemokines and other secreted signalling proteins were measured in the plasma of normal ageing mice using standardized multiplex sandwich enzyme-linked immunosorbent assays (ELISAs; Luminex) (Supplementary Table 1). Using multivariate analysis, we identified seventeen proteins whose levels increased and correlated with decreased neurogenesis during ageing (Fig. 3a and Supplementary Fig. 10a, b). To identify systemic factors associated with heterochronic parabiosis, we analysed plasma samples from young and old mice before and after pairings in an independent proteomic screen. Comparison of young isochronic and heterochronic cohorts identified fifteen factors that increased in heterochronic parabionts (Fig. 3a and Supplementary Fig. 10c), whereas comparison between old isochronic and heterochronic cohorts revealed four factors that decreased in isochronic parabionts (Supplementary Fig. 10c). Interestingly, only six factors—CCL2, CCL11, CCL12, CCL19, haptoglobin and β2-microglobulin—were elevated in old unpaired and young heterochronic cohorts (Fig. 3a). Of these, CCL11 is a chemokine involved in allergic responses and not previously linked to ageing, neurogenesis or cognition. Relative levels of CCL11 were increased in the plasma of mice during normal ageing (Fig. 3b) and in young mice during heterochronic parabiosis (Fig. 3c). Furthermore, we detected an age-related increase in CCL11 in plasma (Fig. 3d) and cerebrospinal fluid (CSF; Fig. 3e), from healthy human individuals between 20 and 90 years of age, suggesting that this age-related systemic increase is conserved across species.

Having identified CCL11 as an age-related systemic factor associated with decreased neurogenesis, we tested its potential biological relevance *in vivo*. We administered CCL11 protein through intraperitoneal injections into young adult Dcx-luciferase reporter mice[20], and using a non-invasive bioluminescent imaging assay detected a significant decrease in neurogenesis (Supplementary Fig. 11b, c). Using immunohistochemical analysis we investigated the effect of systemic CCL11 on adult hippocampal neurogenesis in young adult wild-type mice. We administered CCL11 or vehicle alone, and in combination with either an anti-CCL11 neutralizing antibody or an isotype control antibody through intraperitoneal injections (Fig. 4a). Systemic administration of CCL11 induced an increase in CCL11 plasma levels (Supplementary Fig. 11a), and significantly decreased the number of Dcx-positive cells in the dentate gyrus (Fig. 4b, c). Importantly, this decrease in neurogenesis could be rescued by systemic neutralization of CCL11 (Fig. 4b, c). Likewise, BrdU-positive cells also showed similar changes in cell number (Supplementary Fig. 11d, e), and furthermore

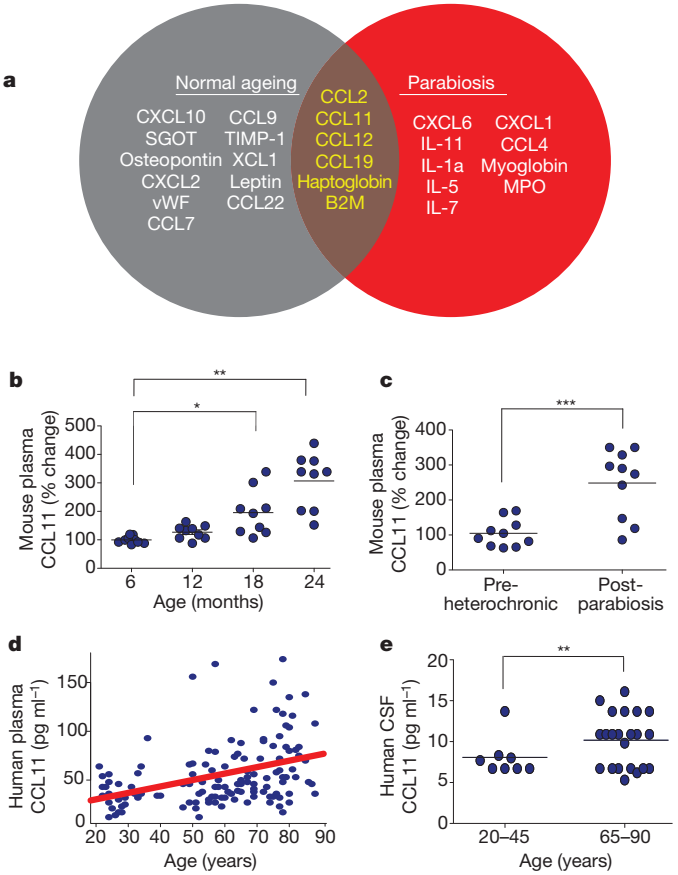

Figure 3 | Systemic chemokine levels increase during ageing and heterochronic parabiosis, and correlate with decreased neurogenesis. **a**, Venn diagram of results from ageing and parabiosis proteomic screens. In grey are shown the seventeen age-related plasma factors that correlated most strongly with decreased neurogenesis, in red are shown the fifteen plasma factors that increased between young isochronic and young heterochronic parabionts, and in the brown intersection are the six factors elevated in both screens. Data from 5–6 mice per age group. **b**, **c**, Changes in plasma concentrations of CCL11 with age (**b**) and young heterochronic parabionts pre- and post- parabiotic pairing (**c**). **d**, **e**, Changes in plasma (**d**; $r = 0.40$; $P = 5.6 \times 10^{-7}$; 95% confidence interval = 0.26–0.53) and CSF (**e**) concentrations of CCL11 with age in healthy human subjects. All data represented as dot plots with mean; $^{*}P < 0.05$; $^{**}P < 0.01$; $^{***}P < 0.001$, *t*-test (**c**, **e**), ANOVA, Tukey's post-hoc test (**a**, **b**), and Mann–Whitney U Test (**d**).

the percentage of cells expressing both BrdU and NeuN decreased (Supplementary Fig. 11f, g). The percentage of cells expressing BrdU and GFAP did not significantly change (Supplementary Fig. 11f, h). As a negative control we assayed neurogenesis after systemic administration of monocyte colony stimulating factor (MCSF), a measured protein whose plasma levels do not change with age, and detected no change in Dcx-positive cells in the dentate gyrus (Supplementary Fig. 12a–d). Together, these data indicate that increasing the systemic level of the age-related factor CCL11 is sufficient to partially recapitulate some of the inhibitory effects observed with ageing and heterochronic parabiosis.

Additionally, we investigated the possibility that age-related blood-borne factors influence neural progenitor activity and neural differentiation *in vitro*. We assayed the number of neurospheres formed after exposure of primary neural stem/progenitor cells (NPCs) to serum from aged mice and observed a 50% decrease when compared to exposure to serum from young mice (Supplementary Fig. 13a). We then tested the effect of CCL11 and observed that the number and size of neurospheres formed from primary NPCs exposed to CCL11 significantly decreased (Supplementary Fig. 13b–d). Using a human-derived NTERA cell line expressing enhanced (e)GFP under the Dcx

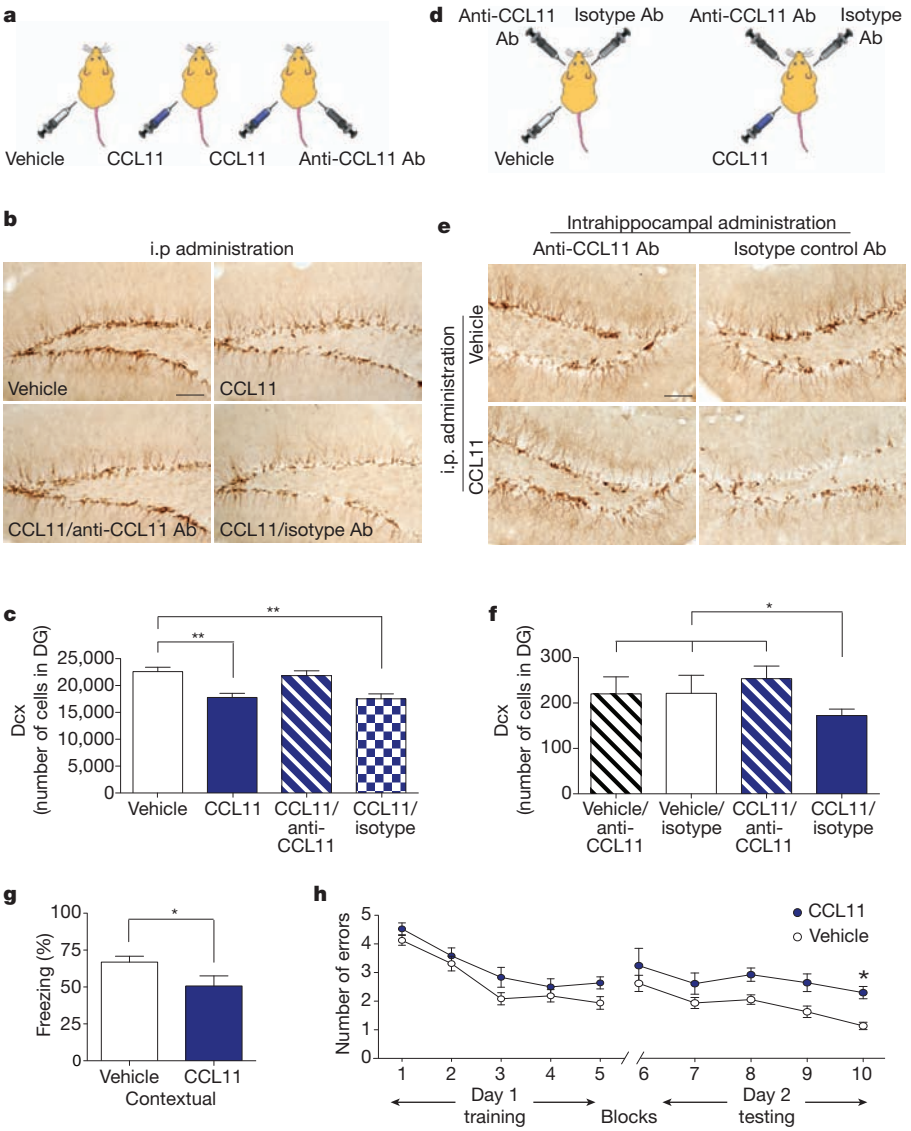

Figure 4 | Systemic exposure to CCL11 inhibits neurogenesis and impairs learning and memory. **a**, Schematic of young (3–4 months) mice injected intraperitoneally with CCL11 or vehicle, and in combination with anti-CCL11 neutralizing or isotype control antibody (Ab). **b**, Representative field of Dcx-positive cells for each treatment group ($n = 6$–10 mice) treated four times over 10 days. i.p., intraperitoneal. Scale bar, 100 μm. **c**, Quantification of neurogenesis in the dentate gyrus after treatment. **d**, Schematic of young adult mice given unilateral stereotaxic injections of anti-CCL11 neutralizing or isotype control antibody followed by systemic injections with either recombinant CCL11 or PBS (vehicle). **e**, Representative field of Dcx-positive cells in adjacent sides of the dentate gyrus for each treatment group ($n = 3$–11 mice). Scale bar, 100 μm. **f**, Quantification of neurogenesis in the dentate gyrus after systemic and stereotaxic treatment. Bars represent mean number of cells in each section. **g**, **h**, Learning and memory assessed by contextual fear conditioning (**g**) and RAWM (**h**) paradigms in young adult mice injected with CCL11 or vehicle every 3 days for 5 weeks ($n = 12$–16 mice per group). All data are represented as mean ± s.e.m.; $*P < 0.05$; $**P < 0.01$; ANOVA, Dunnet's or Tukey's post-hoc test (**c**, **f**); repeated measures ANOVA, Bonferroni post-hoc test (**k**).

promoter, we assayed neural differentiation and observed a significant decrease in eGFP expression after 12 days in culture with CCL11 (Supplementary Fig. 13e, f). Although these findings open the possibility of a direct interaction of systemic factors with progenitor cells *in vivo* during ageing, they do not preclude the possibility of indirect actions by interactions with other neurogenic niche cell types.

To examine the effect of CCL11 on neurogenesis in the brain we stereotaxically injected CCL11 into the dentate gyrus of young adult mice, and observed a decrease in the number of Dcx-positive cells compared with the contralateral dentate gyrus, which received vehicle control (Supplementary Fig. 14a, b). Furthermore, we examined whether the inhibitory effect of peripheral CCL11 could be restored locally within the hippocampus. We stereotaxically injected CCL11-specific neutralizing antibody and isotype control antibodies into the contralateral dentate gyrus of young adult mice (Fig. 4d). After stereotaxic injection, we systemically administered CCL11 or vehicle control by intraperitoneal injections (Fig. 4d). The decrease in Dcx-positive cell number observed in mice that received systemic CCL11 could be rescued by neutralizing CCL11 within the dentate gyrus (Fig. 4e, f), suggesting that the increase in systemic chemokine levels exerts a direct effect in the CNS.

Lastly, to determine the physiological relevance of increased systemic CCL11 levels in mice we assessed hippocampal-dependent learning and memory using contextual fear conditioning and RAWM paradigms (Fig. 4g, h). Young adult mice received intraperitoneal injections of recombinant CCL11 or vehicle control. During fear conditioning training all mice, regardless of treatment, exhibited no differences in baseline freezing (Supplementary Fig. 15a). In contrast, mice that had received CCL11 demonstrated decreased freezing during contextual (Fig. 4g), but not cued (Supplementary Fig. 15b), memory testing. During the training phase of the RAWM task all mice regardless of treatment showed similar swim speeds (Supplementary Fig. 15c) and

learning capacity for the task (Fig. 4h). However, by the end of the testing phase animals that had received CCL11 exhibited impaired learning and memory deficits (Fig. 4h). Together, these functional data demonstrate that increasing the systemic level of CCL11 can not only inhibit adult neurogenesis, but also impair learning and memory.

Cumulatively, our data link age-related molecular changes in the systemic milieu to the age-related decline in adult neurogenesis, and impairments in synaptic plasticity and cognitive function observed during ageing (Supplementary Fig. 1). Whereas local immune signalling in the brain is emerging as a critical modulator of NPC function[11,15,21,22] and neurodegeneration[11,15,21], we now identify systemic immune-related factors as potentially critical contributors to the susceptibility of the ageing brain to cognitive impairments. Interestingly, members of the identified age-related chemokines (CCL2, CCL11 and CCL12) are localized to within 70 kb on mouse chromosome 11, and within 40 kb on human chromosome 17, implicating this genetic locus in normal brain ageing and possibly ageing in general. Indeed, work investigating cellular senescence, a known hallmark of ageing, further suggests the involvement of some of the individual systemic chemokines reported here (CCL2) in the ageing process as components of the senescence-associated secretory phenotype[23]. Lastly, although the proteomic platform we used here was sufficient to identify systemic inhibitory 'ageing' factors it will be critical to develop and utilize broader proteomic screens to facilitate the discovery of systemic pro-neurogenic 'rejuvenating' factors with the potential to ameliorate age-related cognitive dysfunction.

METHODS SUMMARY

Mouse strains used were C57BL/6 (Jackson Laboratory), C57BL/6 aged mice (National Institutes of Ageing), Dcx-Luc[20] and C57BL/6J-Act-GFP (Jackson Laboratory). All animal use was in accordance with institutional guidelines approved by the Veterans Affairs Palo Alto Committee on Animal Research. Parabiosis surgery followed previously described procedures[19] with the addition that peritonea between animals were surgically connected. Immunohistochemistry followed standard published techniques[24]. Extracellular electrophysiology was performed as previously described[25]. Spatial learning and memory was assayed with the RAWM paradigm as previously published[26]. Contextual fear conditioning was assayed as previously published[27]. Relative plasma concentrations of cytokines and signalling molecules in mice and humans were measured using antibody-based multiplex immunoassays at Rules Based Medicine. Statistical analysis was performed with Prism 5.0 software (GraphPad Software). Plasma protein correlations were analysed with the Significance Analysis of Microarray software (*SAM 3.00* algorithm; http://www.stat.stanford.edu/~tibs/SAM/index.htm). Experiments were carried out by investigators blinded to the treatment of animals.

Full Methods and any associated references are available in the online version of the paper at www.nature.com/nature.

Received 3 September 2009; accepted 5 July 2011.

1. van Praag, H., Shubert, T., Zhao, C. & Gage, F. H. Exercise enhances learning and hippocampal neurogenesis in aged mice. *J. Neurosci.* **25,** 8680–8685 (2005).
2. Gage, F. H. Mammalian neural stem cells. *Science* **287,** 1433–1438 (2000).
3. Alvarez-Buylla, A. & Lim, D. A. For the long run: maintaining germinal niches in the adult brain. *Neuron* **41,** 683–686 (2004).
4. Zhao, C., Deng, W. & Gage, F. H. Mechanisms and functional implications of adult neurogenesis. *Cell* **132,** 645–660 (2008).
5. van Praag, H. *et al.* Functional neurogenesis in the adult hippocampus. *Nature* **415,** 1030–1034 (2002).
6. Deng, W., Aimone, J. B. & Gage, F. H. New neurons and new memories: how does adult hippocampal neurogenesis affect learning and memory? *Nature Rev. Neurosci.* **11,** 339–350 (2010).
7. Clelland, C. D. *et al.* A functional role for adult hippocampal neurogenesis in spatial pattern separation. *Science* **325,** 210–213 (2009).
8. Zhang, C. L., Zou, Y., He, W., Gage, F. H. & Evans, R. M. A role for adult TLX-positive neural stem cells in learning and behaviour. *Nature* **451,** 1004–1007 (2008).
9. Saxe, M. D. *et al.* Ablation of hippocampal neurogenesis impairs contextual fear conditioning and synaptic plasticity in the dentate gyrus. *Proc. Natl Acad. Sci. USA* **103,** 17501–17506 (2006).
10. Shen, Q. *et al.* Endothelial cells stimulate self-renewal and expand neurogenesis of neural stem cells. *Science* **304,** 1338–1340 (2004).
11. Carpentier, P. A. & Palmer, T. D. Immune influence on adult neural stem cell regulation and function. *Neuron* **64,** 79–92 (2009).
12. Renault, V. M. *et al.* FoxO3 regulates neural stem cell homeostasis. *Cell Stem Cell* **5,** 527–539 (2009).
13. Molofsky, A. V. *et al.* Increasing $p16^{INK4a}$ expression decreases forebrain progenitors and neurogenesis during ageing. *Nature* **443,** 448–452 (2006).
14. Lie, D. C. *et al.* Wnt signalling regulates adult hippocampal neurogenesis. *Nature* **437,** 1370–1375 (2005).
15. Lucin, K. M. & Wyss-Coray, T. Immune activation in brain aging and neurodegeneration: too much or too little? *Neuron* **64,** 110–122 (2009).
16. Rapp, P. R. & Heindel, W. C. Memory systems in normal and pathological aging. *Curr. Opin. Neurol.* **7,** 294–298 (1994).
17. Ajami, B., Bennett, J. L., Krieger, C., Tetzlaff, W. & Rossi, F. M. Local self-renewal can sustain CNS microglia maintenance and function throughout adult life. *Nature Neurosci.* **10,** 1538–1543 (2007).
18. Bliss, T. V. & Collingridge, G. L. A synaptic model of memory: long-term potentiation in the hippocampus. *Nature* **361,** 31–39 (1993).
19. Conboy, I. M. *et al.* Rejuvenation of aged progenitor cells by exposure to a young systemic environment. *Nature* **433,** 760–764 (2005).
20. Couillard-Despres, S. *et al. In vivo* optical imaging of neurogenesis: watching new neurons in the intact brain. *Mol. Imaging* **7,** 28–34 (2008).
21. Monje, M. L., Toda, H. & Palmer, T. D. Inflammatory blockade restores adult hippocampal neurogenesis. *Science* **302,** 1760–1765 (2003).
22. Moriyama, M. *et al.* Complement receptor 2 is expressed in neural progenitor cells and regulates adult hippocampal neurogenesis. *J. Neurosci.* **31,** 3981–3989 (2011).
23. Fumagalli, M. & d'Adda di Fagagna, F. SASPense and DDRama in cancer and ageing. *Nature Cell Biol.* **11,** 921–923 (2009).
24. Luo, J. *et al.* Glia-dependent TGF-β signaling, acting independently of the TH17 pathway, is critical for initiation of murine autoimmune encephalomyelitis. *J. Clin. Invest.* **117,** 3306–3315 (2007).
25. Xie, X. & Smart, T. G. Modulation of long-term potentiation in rat hippocampal pyramidal neurons by zinc. *Pflugers Arch.* **427,** 481–486 (1994).
26. Alamed, J., Wilcock, D. M., Diamond, D. M., Gordon, M. N. & Morgan, D. Two-day radial-arm water maze learning and memory task; robust resolution of amyloid-related memory deficits in transgenic mice. *Nature Protocols* **1,** 1671–1679 (2006).
27. Raber, J. *et al.* Irradiation enhances hippocampus-dependent cognition in mice deficient in extracellular superoxide dismutase. *Hippocampus* **21,** 72–80 (2011).
28. Brack, A. S. *et al.* Increased Wnt signaling during aging alters muscle stem cell fate and increases fibrosis. *Science* **317,** 807–810 (2007).

Supplementary Information is linked to the online version of the paper at www.nature.com/nature.

Acknowledgements We thank A. Brunet for critically reading the manuscript; M. Buckwalter for parabiosis instruction; T.-T. Huang for irradiation instruction; R. Corniola and C. Clelland for behavioural advice, S. Bauer Huang, H. Johns, J. Sun, H. Hefner, H. Alabsi and I. Villeda for technical assistance. This work was supported by grants from Anonymous (T.W.-C.), Department of Veterans Affairs (T.W.-C.), National Institutes of Health Institute on Aging (R01 AG027505, T.W.-C.), a California Initiative for Regenerative Medicine Award (T.W.-C.), National Institutes of Health (R01 MH078194, X.S.X.), National Institutes of Health Institute on Aging (P30 AG08017, J.A.K.), a National Institutes of Health Director's Pioneer Award (T.A.R.), a Larry L. Hillblom Foundation postdoctoral fellowship (K.M.L.; 2008-A-023-FEL), a Feodor-Lynen postdoctoral fellowship (E.C.), a Swiss National Science Foundation postdoctoral fellowship (A.E.), a National Science Foundation predoctoral fellowship (S.A.V.; K.I.M.; T.M.S.), and Kirschstein NRSA predoctoral fellowships (1 F31 AG034045-01, S.A.V.; 1 F31 NS066676-01A1, Z.D.).

Author Contributions S.A.V. and T.W.-C. developed the concept and designed all experiments. S.A.V. and J.L. designed and performed *in vivo* experiments. S.A.V. performed behavioural experiments. K.I.M. assisted with surgery. B.Z. and X.S.X. performed electrophysiology. M.B. and A.E. analysed human data. G.B. assisted with fear conditioning and irradiation analysis. S.A.V., T.M.S. and J.-S.P. performed *in vitro* experiments. T.M.S. assisted with MCSF analysis. N.F. assisted with radial arm maze. Z.D. performed flow cytometry. K.M.L. performed irradiation. E.C. assisted with *in vivo* plasma experiments. D.R.G., G.L., E.R.P., J.A.K. and J.F.Q. identified aging subjects and provided human samples. S.C.-D. and L.A. provided reagents and mice. T.A.R. provided reagents, conceptual advice and edited the manuscript. S.A.V. collected data, performed data analysis and generated figures. S.A.V. and T.W.-C. wrote the manuscript. T.W.-C. supervised all aspects of this project. All authors had the opportunity to discuss results and comment on the manuscript.

Author Information Reprints and permissions information is available at www.nature.com/reprints. The authors declare no competing financial interests. Readers are welcome to comment on the online version of this article at www.nature.com/nature. Correspondence and requests for materials should be addressed to T.W.-C. (twc@stanford.edu).

METHODS

Mice. The following mouse lines were used: C57BL/6 (The Jackson Laboratory), C57BL/6 aged mice (National Institutes of Ageing), Dcx-Luc mice[20] and C57BL/6J-Act-GFP (Jackson Laboratory). For parabiosis experiments male and female C57BL/6 mouse cohorts were used. For all other *in vivo* pharmacological and behavioural studies young (2–3 months) wild-type C57BL/6 male mice were used. Mice were housed under specific pathogen-free conditions under a 12 h light–dark cycle and all animal handling and use was in accordance with institutional guidelines approved by the Veterans Affairs Palo Alto Committee on Animal Research.

Immunohistochemistry. Tissue processing and immunohistochemistry was performed on free-floating sections following standard published techniques[24]. Briefly, mice were anaesthetized with 400 mg kg^{-1} chloral hydrate (Sigma-Aldrich) and transcardially perfused with 0.9% saline. Brains were removed and fixed in phosphate-buffered 4% paraformaldehyde, pH 7.4, at 4 °C for 48 h before they were sunk through 30% sucrose for cryoprotection. Brains were then sectioned coronally at 40 μm with a cryomicrotome (Leica Camera) and stored in cryoprotective medium. Primary antibodies were: goat anti-Dcx (1:500; Santa Cruz Biotechnology), rat anti-BrdU (1:5,000; Accurate Chemical and Scientific Corp.), goat anti-Sox2 (1:200; Santa Cruz), mouse anti-NeuN (1:1,000; Chemicon), mouse anti-GFAP (1:1,500; DAKO) and mouse anti-CD68 (1:50; Serotec). After overnight incubation, primary antibody staining was revealed using biotinylated secondary antibodies and the ABC kit (Vector) with diaminobenzidine (DAB; Sigma-Aldrich) or fluorescence-conjugated secondary antibodies. For BrdU labelling, brain sections were pre-treated with 2 N HCl at 37 °C for 30 min before incubation with primary antibody. For double-label immunofluorescence of BrdU/NeuN or BrdU/GFAP, sections were incubated overnight with rat anti-BrdU, rinsed and incubated for 1 h with donkey anti-rat antibody (2.5 μg ml^{-1}; Vector) before they were stained with mouse anti-NeuN antibody. To estimate the total number of Dcx- or Sox2-positive cells per dentate gyrus immunopositive cells in the granule cell and subgranular cell layer of the dentate gyrus were counted in every sixth coronal hemibrain section through the hippocampus and multiplied by 12.

BrdU administration and quantification of BrdU-positive cells. 50 mg kg^{-1} of BrdU was injected intraperitoneally into mice once a day for 6 days, and mice were killed 28 days later or injected daily for 3 days before being killed. To estimate the total number of BrdU-positive cells in the brain, we performed DAB staining for BrdU on every sixth hemibrain section. The number of BrdU-positive cells in the granule cell and subgranular cell layer of the dentate gyrus were counted and multiplied by 12 to estimate the total number of BrdU-positive cells in the entire dentate gyrus. To determine the fate of dividing cells a total of 200 BrdU-positive cells across 4–6 sections per mouse were analysed by confocal microscopy for co-expression with NeuN and GFAP. The number of double-positive cells was expressed as a percentage of BrdU-positive cells.

Parabiosis and flow cytometry. Parabiosis surgery followed previously described procedures[19]. Pairs of mice were anaesthetized and prepared for surgery. Mirror-image incisions at the left and right flanks, respectively, were made through the skin. Shorter incisions were made through the abdominal wall. The peritoneal openings of the adjacent parabionts were sutured together. Elbow and knee joints from each parabiont were sutured together and the skin of each mouse was stapled (9-mm autoclip, Clay Adams) to the skin of the adjacent parabiont. Each mouse was injected subcutaneously with Baytril antibiotic and Buprenex as directed for pain and monitored during recovery. Flow cytometric analysis was done on fixed and permeabilized blood plasma cells from GFP and non-GFP parabionts. Approximately 40–60% of cells in the blood of either parabiont were GFP-positive 2 weeks after parabiosis surgery. We observed 70–80% survival rate in parabionts 5 weeks after parabiosis surgery.

Extracellular electrophysiology. Acute hippocampal slices (400-μm thick) were prepared from unpaired and young parabionts. Slices were maintained in artificial cerebrospinal fluid (ACSF) continuously oxygenated with 5% CO_2/95% O_2. ACSF composition was as follows: (in mM): NaCl 124.0; KCl 2.5; KH_2PO_4 1.2; $CaCl_2$ 2.4; $MgSO_4$ 1.3; $NaHCO_3$ 26.0; glucose 10.0 (pH 7.4). Recordings were performed with an Axopatch- 2B amplifier and pClamp 10.2 software (Axon Instruments). Submerged slices were continuously perfused with oxygenated ACSF at a flow rate of 2 ml min^{-1} from a reservoir by gravity feeding. Field potential (population spikes and EPSPs) was recorded using glass microelectrodes filled with ACSF (resistance: 4–8 MΩ). Biphasic current pulses (0.2 ms duration for one phase, 0.4 ms in total) were delivered in 10-s intervals through a concentric bipolar stimulating electrode (FHC). No obvious synaptic depression or facilitation was observed with this frequency stimulation. To record field population spikes in the dentate gyrus, the recording electrode was placed in the lateral or medial side of the dorsal part of the dentate gyrus. The stimulating electrode was placed right above the hippocampal fissure to stimulate the perforant pathway fibres. Signals were filtered at 1 KHz and digitized at 10 KHz. Tetanic stimulation consisted of 2 trains of 100 pulses (0.4 ms pulse duration, 100 Hz) delivered with an inter-train interval of 5 s. The amplitude of the population spike was measured from the initial phase of the negative wave. Up to five consecutive traces were averaged for each measurement. Synaptic transmission was assessed by generating input–output curves, with stimulus strength adjusted to be ~30% of the maximum. LTP was calculated as mean percentage change in the amplitude of the population spike following high-frequency stimulation relative to its basal amplitude.

Contextual fear conditioning. The paradigm was done following previously published techniques[27]. In this task, mice learned to associate the environmental context (fear-conditioning chamber) with an aversive stimulus (mild foot shock; unconditioned stimulus (US)), enabling testing for hippocampal-dependent contextual fear conditioning. As contextual fear conditioning is hippocampus and amygdala dependent, the mild foot shock was paired with a light and tone cue (conditioned stimulus (CS)) in order to also assess amygdala-dependent cued fear conditioning. Conditioned fear was displayed as freezing behaviour. Specific training parameters are as follows: tone duration is 30 s; level is 70 dB, 2 kHz; shock duration is 2 s; intensity is 0.6 mA. This intensity is not painful and can easily be tolerated but will generate an unpleasant feeling. More specifically, on day 1 each mouse was placed in a fear-conditioning chamber and allowed to explore for 2 min before delivery of a 30 s tone (70 dB) ending with a 2 s foot shock (0.6 mA). Two minutes later, a second CS–US pair was delivered. On day 2 each mouse was first place in the fear-conditioning chamber containing the same exact context, but with no adminstration of a CS or foot shock. Freezing was analysed for 1–3 min. One hour later, the mice were placed in a new context containing a different odour, cleaning solution, floor texture, chamber walls and shape. Animals were allowed to explore for 2 min before being re-exposed to the CS. Freezing was analysed for 1–3 min. Freezing was measured using a FreezeScan video tracking system and software (Cleversys).

RAWM. Spatial learning and memory was assessed using the RAWM paradigm following the exact protocol described previously[26]. The goal arm location containing a platform remains constant throughout the training and testing phase, whereas the start arm is changed during each trial. On day 1 during the training phase, mice are trained for 15 trials, with trials alternating between a visible and hidden platform. On day 2 during the testing phase, mice are tested for 15 trials with a hidden platform. Entry into an incorrect arm is scored as an error, and errors are averaged over training blocks (three consecutive trials).

Cranial irradiation. Adult mice (8–12 weeks) were sham irradiated (controls) or irradiated at 5 Gy three times over 8 days using the Mark I gamma irradiator and killed at 8–10 weeks after irradiation to collect brains for immunohistochemical analyses. Each mouse was placed in a restrainer that was fitted into a slot in the lead brick shield so that the back of the skull was facing the source of radiation when positioned in the radiation chamber. The shield is constructed of lead bricks such that only the hippocampal/midbrain area was exposed to radiation. Calibration for 5 Gy radiation was done using nanoDot. Shielded areas were protected with an exposure rate ten times lower than the exposed area. RAWM studies were done on irradiated mice at least 6 weeks after the radiation procedure. This time frame ensured adequate recovery of the animals. All data were from 8 irradiated and 10 sham-irradiated mice.

Plasma collection and proteomic analysis. Mouse blood was collected from 400–500 young (2–3 months) and old (18–22 months) animals into EDTA-coated tubes via tail vein bleed, mandibular vein bleed, or intracardial bleed at time of death. EDTA plasma was generated by centrifugation of freshly collected blood and aliquots were stored at −80 °C until use. Human plasma and CSF samples were obtained from academic centres and subjects were chosen based on standardized inclusion and exclusion criteria as previously described[29,30]. The relative plasma concentrations of cytokines and signalling molecules were measured in human and mouse plasma samples using standard antibody-based multiplex immunoassays (Luminex) by either Rules Based Medicine, a fee-for-service provider, or by the Human Immune Monitoring Center at Stanford University. All Luminex measurements where obtained in a blinded fashion. All assays were developed and validated to Clinical Laboratory Standards Institute (formerly NCCLS) guidelines based upon the principles of immunoassay as described by the manufacturers.

CCL11, MSCF, antibody, or plasma administration. Carrier-free recombinant murine CCL11 dissolved in PBS (10 μg kg^{-1}; R&D Systems), carrier-free recombinant MCSF dissolved in PBS (10 μg kg^{-1}; Biogen), rat IgG2a neutralizing antibody against mouse CCL11 (50 μg kg^{-1}; R&D Systems, clone 42285), and isotype-matched control rat IgG2a recommended by the manufacturer (R&D Systems, clone 54447) were administered systemically via intraperitoneal injection over ten days on day 1, 4, 7 and 10. The same reagents (0.50 μl; 0.1 μg μl^{-1}) were also administered stereotaxically into the dentate gyrus of the hippocampus in some experiments (coordinates from bregma: $A = -2.0$ mm and $L = -1.8$ mm; from brain surface: $H = -2.0$ mm). Pooled mouse serum or plasma was collected from young (2–3 months) mice and old (18–20 months) mice by intracardial bleed at time of death. Serum was prepared from clotted blood collected without anticoagulants;

plasma was prepared from blood collected with EDTA followed by centrifugation. Aliquots were stored at −80 °C until use. Prior to administration plasma was dialysed in PBS to remove EDTA. Young adult mice were systemically treated with plasma (100 µl) isolated from young or aged mice via intravenous injections four times over 10 days.

***In vivo* bioluminescence imaging.** Bioluminescence was detected with the *In vivo* Imaging System (IVIS Spectrum; Caliper Life Science). Mice were injected intraperitoneally with 150 mg kg^{-1} D-luciferin (Xenogen) 10 min before imaging and anaesthetized with isofluorane during imaging. Photons emitted from living mice were acquired as photons per second per cm^2 per steridan (sr) using LIVINGIMAGE software (version 3.5, Caliper) and integrated over 5 min. For quantification a region of interest was manually selected and kept constant for all experiments.

Cell culture assays. Mouse NPCs were isolated from C57BL/6 mice as previously described[12]. Brains from postnatal animals (1-day old) were dissected to remove the olfactory bulb, cerebellum and brainstem. After removing superficial blood vessels forebrains were finely minced, digested for 30 min at 37 °C in DMEM media containing 2.5 U ml^{-1} Papain (Worthington Biochemicals), 1 U ml^{-1} Dispase II (Boeringher Mannheim) and 250 U ml^{-1} DNase I (Worthington Biochemicals) and mechanically dissociated. NPCs were purified using a 65% Percoll gradient and plated on uncoated tissue culture dishes at a density of 10^5 cells cm^{-2}. NPCs were cultured under standard conditions in NeuroBasal A medium supplemented with penicillin (100 U ml^{-1}), streptomycin (100 mg ml^{-1}), 2 mM L-glutamine, serum-free B27 supplement without vitamin A (Sigma-Aldrich), bFGF (20 ng ml^{-1}) and EGF (20 ng ml^{-1}). Carrier-free forms of murine recombinant CCL11 (100 ng ml^{-1}, R&D Systems), goat IgG neutralizing antibody against mouse CCL11 (10 µg ml^{-1}; R&D Systems), and control goat IgG (10 µg ml^{-1}; R&D Systems) were dissolved in PBS and added to cell cultures under self-renewal conditions every other day following cell plating.

Human NTERA cells[7] expressing eGFP under the Dcx promoter were cultured under standard self-renewal and differentiation conditions[31,32]. Carrier-free forms of human recombinant CCL11 (100 ng ml^{-1}, R&D Systems), mouse IgG_1 neutralizing antibody against human CCL11 (25 µg ml^{-1}; R&D Systems, clone 43911) and control mouse IgG_1 (25 µg ml^{-1}; R&D Systems) were added to cell cultures under differentiation conditions every other day following cell plating.

Data and statistical analysis. Data are expressed as mean ± s.e.m. Statistical analysis was performed with Prism 5.0 software (GraphPad Software). Means between two groups were compared with two-tailed, unpaired Student's *t*-test. Comparisons of means from multiple groups with each other or against one control group were analysed with one-way ANOVA and Tukey-Kramer's or Dunnett's post-hoc tests, respectively. Plasma protein correlations in the ageing samples were analysed with the Significance Analysis of Microarray software (*SAM 3.00* algorithm; http://www.stat.stanford.edu/~tibs/SAM/index.htm). Unsupervised cluster analysis was performed using Gene Cluster 3.0 software and node maps were produced using Java TreeView 1.0.13 software. All histology, electrophysiology and behaviour experiments conducted were done in a randomized and blinded fashion.

29. Zhang, J. *et al.* CSF multianalyte profile distinguishes Alzheimer and Parkinson diseases. *Am. J. Clin. Pathol.* **129,** 526–529 (2008).
30. Li, G. *et al.* Cerebrospinal fluid concentration of brain-derived neurotrophic factor and cognitive function in non-demented subjects. *PLoS ONE* **4,** e5424 (2009).
31. Couillard-Despres, S. *et al.* Human *in vitro* reporter model of neuronal development and early differentiation processes. *BMC Neurosci.* **9,** 31 (2008).
32. Buckwalter, M. S. *et al.* Chronically increased transforming growth factor-β1 strongly inhibits hippocampal neurogenesis in aged mice. *Am. J. Pathol.* **169,** 154–164 (2006).